

湍流烟传递方程及其应用

王松平¹, 陈清林², 华 贵²

(1. 青岛大学师范学院物理系, 山东 青岛 266071;

2. 华南理工大学 教育部强化传热与过程节能重点实验室, 广东 广州 510641)

摘要: 导出了湍流烟传递方程组, 依此研究了壁面常热流对流换热管的烟传递, 计算了由于粘性耗散、径向和轴向导热引起的烟损率分布。通过对单位体积总烟损率的计算表明, 单位体积总烟损率是换热管几何参数和边界条件的多元函数, 对于给定的几何参数, 存在使单位体积总烟损率最小的边界条件, 反之亦然。该结论对优化设计换热器及对给定边界条件的换热器优化选取具有一定的指导意义。

关键词: 湍流; 烟传递方程; 烟损率分布

中图分类号: TK123

文献标识码: A

1 引言

能量的传递和转换必然伴随其“质”—烟的传递和转换。能量在传递和转换过程中其量守恒, 而烟在传递和转换过程中其量不守恒。因此, 烟必有其独特的传递和转换规律。近年来对烟传递规律的研究已取得了一些进展^{1~4}。作为更一般的研究, 文献[4]导出了描述烟传递规律的一般方程组, 并在层流的情况给出求解烟传递基本方程组的方法。本文将研究湍流烟传递, 首先利用 Reynolds 时均方法导出湍流烟传递方程组, 然后依此研究壁面常热流对流换热管的烟传递规律。

2 湍流烟传递方程组

考虑充分发展的不可压缩的单组分牛顿流体, 略去外力的作用和湍流能量耗散项, 且考虑常物性, 则对描述连续流体运动的烟传递方程组^[4]取 Reynolds 时均可得湍流烟传递方程组:

$$\frac{\partial V_i}{\partial x_i} = 0, \frac{\partial V'_i}{\partial x_i} = 0 \quad (1)$$

$$\rho \frac{\partial V_i}{\partial t} + \rho V_j \frac{\partial V_i}{\partial x_j} = - \frac{\partial p}{\partial x_i} + \mu \frac{\partial^2 V_i}{\partial x_j^2} -$$

$$\frac{\partial(-\rho \overline{V'_i V'_j})}{\partial x_j} \quad (2)$$

$$\rho C_p \frac{\partial T}{\partial t} + \rho C_p \frac{\partial}{\partial x_i} (T \overline{V}_i) = -k_q \frac{\partial^2 T}{\partial x_i \partial x_i} + \Phi -$$

$$\rho C_p \frac{\partial}{\partial x_i} (\overline{T' V'_j}) \quad (3)$$

$$\frac{\partial}{\partial x_i} (\rho \overline{ex V}_i + \overline{j_{ex, i}}) = -\overline{d_{ex}} \quad (4)$$

$$\overline{j_{ex, i}} = (\overline{P_{ij}} - p_0 \overline{\delta}_{ij}) \overline{V}_j + \left(1 - \frac{T_0}{T}\right) \frac{\partial T}{\partial x_i} + \overline{P'_{ij} V'_j} \quad (5)$$

$$\overline{d_{ex}} = T_0 \left[\frac{2\mu}{T} \overline{S_{ji} S_{ij}} + \frac{k_q}{T^2} \frac{\partial T}{\partial x_i} \frac{\partial T}{\partial x_i} + \frac{2\mu}{T} \overline{S'_{ji} S'_{ij}} + \frac{k_q}{T^2} \frac{\partial T'}{\partial x_i} \frac{\partial T'}{\partial x_i} \right] \quad (6)$$

对于定常、均匀湍流剪切流, 由于湍流的统计状态是定常、均匀的, 即不随时间和空间变化的, 则式(6)简化为:

$$\overline{d_{ex}} = T_0 \left[\frac{2\mu}{T} \overline{S_{ij} S_{ij}} + \frac{k_q}{T^2} \frac{\partial T}{\partial x_i} \frac{\partial T}{\partial x_i} - \frac{1}{T} \rho \overline{V'_i V'_j} \overline{S_{ij}} - \frac{1}{T^2} C_p \rho \overline{T' V'_j} \frac{\partial T}{\partial x_j} \right] \quad (7)$$

式中, $\overline{d_{ex}}$ 为烟损率的时均值, $\overline{j_{ex, i}}$ 为烟流时均值。下面将以实例研究方程组的求解和应用。

3 壁面常热流的管内湍流烟传递

研究壁面常热流的管内充分发展的单组分流体的湍流烟传递, 需要求解方程(1)~(7)。为求解式(1)~式(3), 我们应用 Prandtl 混合长度理论模型, Reynolds 应力 $-\rho \overline{V'_i V'_j}$ 和湍流能流项 $-\rho C_p \overline{V'_i V'_j}$ 可用 Deissler 表达式^[5]:

收稿日期: 2000-01-24; 修订日期: 2000-09-21

基金项目: 国家重点基础研究发展规划基金资助项目(G2000026307)

作者简介: 王松平(1959-)男, 山东日照人, 青岛大学师范学院副教授

$$\rho \overline{V_i V_j} = \begin{cases} -2n^2 \rho l |\overline{V_i} - V_{(s)i}| \left\{ 1 - \exp\left[-n^2 \rho l |\overline{V_i} - V_{(s)i}| / \mu\right] \right\} \overline{S_{ij}} + \frac{2}{3} K \delta_{ij} \text{ (对粘性底层和缓冲层)} \\ -2\eta_1^* \rho l^2 \sqrt{2\text{tr}[S_{ij}]^2} \overline{S_{ij}} + \frac{2}{3} K \delta_{ij} \text{ (对充分发展湍流区)} \end{cases} \quad (8)$$

$$c \rho \overline{T' V_i} = \begin{cases} -n^2 \rho C_p l |\overline{V_i} - V_{(s)i}| \left\{ 1 - \exp\left[-n^2 \rho l |\overline{V_i} - V_{(s)i}| / \mu\right] \right\} \frac{\partial T}{\partial x_i} \text{ (对粘性底层和缓冲层)} \\ -\eta_1^* \rho C_p l^2 \sqrt{2\text{tr}[S_{ij}]^2} \frac{\partial T}{\partial x_i} \text{ (对充分发展湍流区)} \end{cases} \quad (9)$$

其中, $K = \overline{V_i V_i} / 2$, $\eta_1^* = (0.36)^2$ 为 Prandtl 常数, $n = \rho V^* R / \mu \gg 1$ 的湍流流动, 平均速度和平均温度 $= 0.124$ 为 Deissler 数, $V_{(s)i}$ 为壁面速度. 考虑 $N_{(1)}$ 可采用 Deissler 的结果^[3]:

$$V_z^+ = \begin{cases} \int_0^{l^+} \frac{dl^+}{1 + (0.124)^2 V_z^+ l^+ [1 - \exp(- (0.124)^2 V_z^+ l^+)]} \text{ (} 0 \leq l^+ \leq 26, \text{对粘性底层和缓冲层)} \\ \frac{1}{0.36} \ln l^+ + 3.8 \text{ (} l^+ > 26, \text{对充分发展湍流区)} \end{cases} \quad (10)$$

$$T^+ = \begin{cases} - \int_0^{l^+} \frac{dl^+}{1/Pr + (0.24)^2 V_z^+ l^+ [1 - \exp(- (0.124)^2 V_z^+ l^+)]} \text{ (} 0 \leq l^+ \leq 26, \text{对粘性底层和缓冲层)} \\ - \frac{1}{0.36} \ln(l^+ / 26) + T^+ (l^+ = 26) \text{ (} l^+ > 26, \text{对充分发展湍流区)} \end{cases} \quad (11)$$

其中, $V_z^+ = V_z / V^*$ 为无维速度, $V^* = \sqrt{\tau_w / \rho}$ 为摩擦速度, τ_w 为壁面切应力, $l^+ = (R-r) \rho V^* / \mu$ 为距壁面的无维距离, $T^+ = \rho C_p V^* (T - T_w) / j_{qw}$ 为无维温度, T_w 为壁面温度, j_{qw} 为壁面常热流. 将式(8) ~

(11) 代入式(7), 并由于 $\overline{S_{ij}}$ 只有一个分量, $\overline{S_{rz}} = \overline{S_{rz}} = \frac{1}{2} \frac{d\overline{V_z}}{dr}$ 和对均匀常热流有 $\frac{\partial T(r, z)}{\partial z} = \frac{dT_w}{dz} = \frac{dT_{av}}{dz} = \frac{2j_{qw}}{\rho C_p V_{av} R} = \text{常量}^{[6]}$, 得火损率的分布为:

$$\begin{aligned} \overline{d_{ex}} \text{ (粘性底层和缓冲层)} &= \overline{d_{ex, v}} + \overline{d_{ex, rR}} + \overline{d_{ex, rZ}} \\ &= \frac{T_0 \rho^2 V^{*4}}{\mu T_w} \left\{ T^+ / B_{wT} + 1 \right\}^{-1} \left\{ 1 + n^2 l^+ V_z^+ [1 - \exp(-n^2 l^+ V_z^+)] \right\}^{-1} \\ &\quad + \frac{T_0 Pr C_p \rho^2 V^{*2}}{B_{wT}^2 \mu} \left\{ T^+ / B_{wT} + 1 \right\}^{-2} \left\{ 1 + n^2 l^+ V_z^+ Pr [1 - \exp(-n^2 l^+ V_z^+)] \right\}^{-1} \\ &\quad + \frac{4T_0 \mu C_p \phi}{(RB_{wT})^2 Pr} \left\{ T^+ / B_{wT} + 1 \right\}^{-2} \left\{ 1 + n^2 l^+ V_z^+ Pr [1 - \exp(-n^2 l^+ V_z^+)] \right\} \end{aligned} \quad (12)$$

$$\begin{aligned} \overline{d_{ex}} \text{ (充分发展湍流区)} &= \overline{d_{ex, v}} + \overline{d_{ex, rR}} + \overline{d_{ex, rZ}} = \frac{T_0 \rho^2 V^{*4}}{\mu T_w} \left\{ T^+ / B_{wT} + 1 \right\}^{-1} \left\{ 1 + \eta_1^* l^+ / 0.36 \right\} \left(0.36 l^+ \right)^{-2} \\ &\quad + \frac{T_0 Pr C_p \rho^2 V^{*2}}{B_{wT}^2 \mu} \left\{ T^+ / B_{wT} + 1 \right\}^{-2} \left\{ 1 + \eta_1^* l^+ Pr / 0.36 \right\} \left(0.36 Pr l^+ \right)^{-2} \\ &\quad + \frac{4T_0 \mu C_p \phi}{(RB_{wT})^2 Pr} \left\{ T^+ / B_{wT} + 1 \right\}^{-2} \left\{ 1 + \eta_1^* l^+ Pr / 0.36 \right\} \end{aligned} \quad (13)$$

式中, $\phi = (V^* / V_{av})^2$ 为摩擦系数. 定义粘性无维火损率 $d_v^+ = \frac{\mu T_w}{T_0 \rho^2 V^{*4}} \overline{d_{ex, v}}$, 径向导热无维火损率 $d_{rR}^+ = \frac{B_{wT}^2 \mu}{T_0 Pr C_p \rho^2 V^{*2}} \overline{d_{ex, rR}}$, 轴向导热无维火损率 $d_{rZ}^+ = \frac{(RB_{wT})^2 Pr}{4T_0 \mu C_p \phi} \overline{d_{ex, rZ}}$; 则对粘性底层和缓冲层有:

$$d_v^+ = \left\{ T^+ / B_{wT} + 1 \right\}^{-1} \left\{ 1 + n^2 l^+ V_z^+ [1 - \exp(-n^2 l^+ V_z^+)] \right\}^{-1} \quad (14)$$

$$d_{rR}^+ = \left\{ T^+ / B_{wT} + 1 \right\}^{-2} \left\{ 1 + n^2 l^+ V_z^+ Pr [1 - \exp(-n^2 l^+ V_z^+)] \right\}^{-1} \quad (15)$$

$$d_{rZ}^+ = \left\{ T^+ / B_{wT} + 1 \right\}^{-2} \left\{ 1 + n^2 l^+ V_z^+ Pr [1 - \exp(-n^2 l^+ V_z^+)] \right\} \quad (16)$$

对充分发展的湍流区有:

$$d_v^+ = \left\{ T^+ / B_{wT} + 1 \right\}^{-1} \left\{ 1 + \eta_1^* l^+ / 0.36 \right\} \quad (17)$$

$$d_{TR}^+ = \left\{ T^+ / B_{wT} + 1 \right\}^{-2} \left\{ 1 + \eta_1^* l^+ Pr / 0.36 \right\} \quad (18)$$

$$d_{TZ}^+ = \left\{ T^+ / B_{wT} + 1 \right\}^{-2} \left\{ 1 + \eta_1^* l^+ Pr / 0.36 \right\} \quad (19)$$

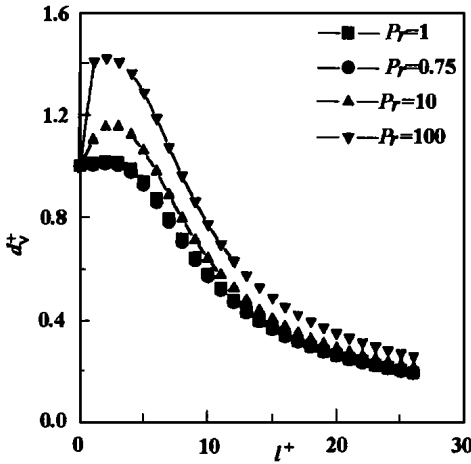


图 1 粘性底层和缓冲层火焰损失率分布 ($B_{wT} = 100$)

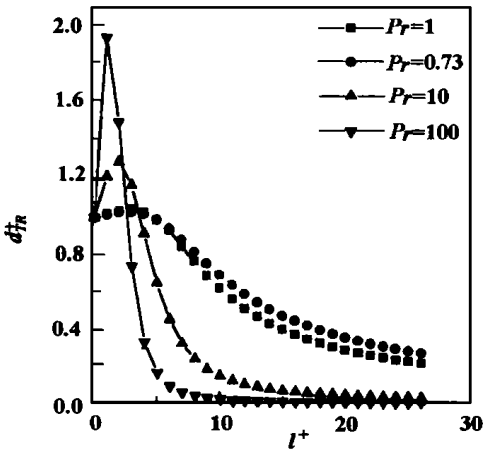


图 2 径向导热火焰损失率分布 ($B_{wT} = 100$)

由式 (10)、式 (11) 和式 (14) ~ (19) 可看出, 无维火焰损失率是以 B_{wT} 、 Pr 为参量, 随 l^+ 变化的函数。在不同的参量 Pr 下, 在粘性底层和缓冲层, 无维火焰损失率的空间分布 (14) ~ (16) 表明在图 1 ~ 图 3。从图中看出, 粘性火焰损失率和径向导热的火焰损失率主要集中于粘

性底层和缓冲层, 火焰损失率最大位置并非近壁面处, 这

$$\begin{aligned} \overline{d_{ex}} (\text{粘性底层和缓冲层}) &= \frac{T_0 \mu^3 \phi^2 Re^4}{T_w \rho^2 D^4} \left\{ \frac{j_{qw} DT^+}{C_p \mu T_w Re \phi^{1/2}} + 1 \right\}^{-1} \left\{ 1 + n^2 l^+ V_z^+ [1 - \exp(-n^2 l^+ V_z^+)] \right\}^{-1} \\ &+ \frac{T_0 j_{qw}^2 Pr}{\mu C_p T_w^2} \left\{ \frac{j_{qw} DT^+}{C_p \mu T_w Re \phi^{1/2}} + 1 \right\}^{-2} \left\{ 1 + n^2 l^+ V_z^+ Pr [1 - \exp(-n^2 l^+ V_z^+)] \right\}^{-1} \\ &+ \frac{16 T_0 j_{qw}^2}{\mu C_p T_w^2 Re^2 Pr} \left\{ \frac{j_{qw} DT^+}{C_p \mu T_w Re \phi^{1/2}} + 1 \right\}^{-2} \left\{ 1 + n^2 l^+ V_z^+ Pr [1 - \exp(-n^2 l^+ V_z^+)] \right\} \quad (20) \end{aligned}$$

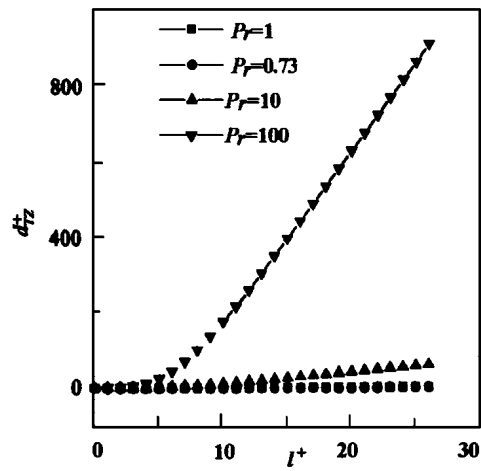


图 3 轴向导热火焰损失率分布 ($B_{wT} = 100$)

是由于粘性火焰损失率与粘性耗散成正比, 而与温度成反比, 径向导热火焰损失率与温度梯度的平方成正比, 而与温度的平方成反比。在充分发展的湍流区,

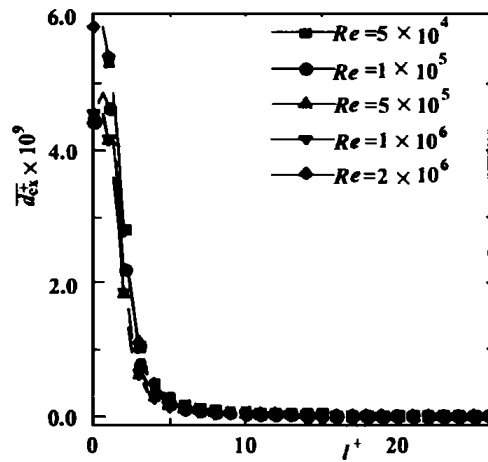


图 4 粘性底层和缓冲层总火焰损失率分布

无维火焰损失率的空间分布规律由式 (17) ~ 式 (19) 容易得出, 在这一区域的火焰损失率相对较小。

4 单位体积的总火焰损失率

下面进一步考虑单位体积的总火焰损失率。由于平均速度 V_w 可通过式 (10) 得到, 所以 ϕ 可以求得。在此应用 Schlichting 公式^[7] $\phi = 1.0 / [2.456 \ln(Re \phi^{1/2}) - 0.29]^2$, 则式 (12)、式 (13) 可改写为:

$$\begin{aligned} \overline{d_{ex}}(\text{充分发展湍流区}) &= \frac{T_0 \mu^3 \phi^2 Re^4}{T_w \rho^2 D^4} \left\{ \frac{j_{qw} DT^+}{C_p \mu T_w Re \phi^{1/2}} + 1 \right\}^{-1} \left\{ 1 + \eta_l^* l^+ / 0.36 \right\} (0.36 l^+)^{-2} \\ &+ \frac{T_0 j_{qw}^2 Pr}{\mu C_p T_w^2} \left\{ \frac{j_{qw} DT^+}{C_p \mu T_w Re \phi^{1/2}} + 1 \right\}^{-2} \left\{ 1 + \eta_l^* l^+ Pr / 0.36 \right\} (0.36 Pr l^+)^{-2} \\ &+ \frac{16 T_0 j_{qw}^2}{\mu C_p T_w^2 Re^2 Pr} \left\{ \frac{j_{qw} DT^+}{C_p \mu T_w Re \phi^{1/2}} + 1 \right\}^{-2} \left\{ 1 + \eta_l^* l^+ Pr / 0.36 \right\} \end{aligned} \quad (21)$$

从式(20)和式(21)看出,若流体确定,则 $\overline{d_{ex}}$ 损率为 Re, D, l^+, T_w, j_{qw} 的函数,即

$$\overline{d_{ex}} = \overline{d_{ex}}(Re, D, l^+, T_w, j_{qw}) \quad (22)$$

对确定的几何参数 D 和给定的边界条件 Re, T_w, j_{qw} , 则式(22)给出单位体积总 $\overline{d_{ex}}$ 损率的径向分布规律。以水为例,取 $D = 0.05 \text{ m}$, $T_w = 330 \text{ K}$, $j_{qw} = 3 \times 10^6 \text{ J} \cdot \text{m}^{-2} \cdot \text{s}^{-1}$ 和不同的 Re , 其粘性底层和缓冲层单位体积总 $\overline{d_{ex}}$ 损率分布表明在图4。从图中可见,对不同的 Re 其 $\overline{d_{ex}}$ 损率分布不同,并且存在一个使 $\overline{d_{ex}}$ 损率分布最小的 Re 。对充分发展的湍流区,可根据式(21)作出单位体积总 $\overline{d_{ex}}$ 损率分布曲线,在这一区域的 $\overline{d_{ex}}$ 损率相对较小。

式(22)对 l^+ 积分可得单位长度的 $\overline{d_{ex}}$ 损率为:

$$\overline{d_{ex}}(Re, D, T_w, j_{qw}) = \int_0^{\sqrt{Re}/2} 2\pi \left(\frac{1}{2} - \frac{l^+}{Re \phi^{1/2}} \right) \frac{D^2}{Re \phi^{1/2}} dl^+ \quad (39)$$

在 $\overline{d_{ex}}(Re, D, T_w, j_{qw})$ 中,独立的几何参数是 D , 边界条件是 Re, T_w, j_{qw} , 根据工程的需要,对给定不同的边界条件,可选择几何参数以使单位长度的 $\overline{d_{ex}}$ 损率最小。

5 结论

上述针对湍流流动的情况,应用 Reynolds 时均方法导出了湍流 $\overline{d_{ex}}$ 传递的方程组,依此研究了壁面常热流对流换热管的 $\overline{d_{ex}}$ 传递,给出了由于粘性耗散、径向和轴向导热引起的 $\overline{d_{ex}}$ 损率分布,及粘性耗散和导热引起的单位体积总 $\overline{d_{ex}}$ 损率分布,结果表明:

(1) 求解湍流 $\overline{d_{ex}}$ 传递方程组比平均体积计算方

法^[8-9]更细致地给出了实际过程的 $\overline{d_{ex}}$ 损率分布规律,揭示了由于不同机理引起 $\overline{d_{ex}}$ 损失的大小及位置所在。

(2) 单位体积总 $\overline{d_{ex}}$ 损率是换热管几何参数和边界条件的多元函数,对于给定的几何参数,存在使单位体积总 $\overline{d_{ex}}$ 损率最小的边界条件,反之亦然。这对优化设计换热器及对给定边界条件的换热器优化选取具有一定的指导意义。

参考文献:

- [1] SOMA J. Exergy transfer: A new field of energy endeavor[J]. **Energy Engineering**, 1985, **82**(4): 11-12.
- [2] XIANG Xin-yao, CHENG Qing-lin. The exergy transfer equation and drive work in steady-state region of site combustion drive oil[C]. **Proceedings of International Symposium on TAIES**, 1997. 91-95.
- [3] CARRINGTON C G, SUN Z F. Exergy balance in turbulent flows [A]. ECOS '92 International Symposium on Efficiency, Cost Optimization and Simulation[C]. New York: Published by ASME, 1992. 521-528.
- [4] 王松平,尹清华,陈清林等. $\overline{d_{ex}}$ 传递—基础理论研究[J]. 华南理工大学学报, 1998, **26**(6): 30-36.
- [5] SLATTERY J C. Momentum, energy and mass transfer in continua [M]. New York: McGraw Hill Inc., 1978.
- [6] 费祥麟. 高等流体力学[M]. 西安: 西安交通大学出版社, 1989.
- [7] SCHLICHTING H. Boundary-Layer Theory[M]. 7th Edition. McGraw-Hill Book Company, 1979.
- [8] BEJAN A. A study of entropy generation in fundamental convective heat transfer[J]. **Journal of Heat Transfer**, 1979, **101**: 718-725.
- [9] SAN J Y. Entropy generation in combined heat and mass transfer[J]. **International Journal of Heat and Mass Transfer**, 1987, **30**(7): 1359-1369.

(何静芳 编辑)

欢迎订阅《热能动力工程》期刊

Technology, Harbin, China, Post Code: 150001) // Journal of Engineering for Thermal Energy & Power. — 2001, 16(1). — 70 ~ 72

A mathematical model was set up for an asymmetrical rotor-bearing system. With the help of this model the authors have analyzed the influence of a variety of factors on the stability of the asymmetrical rotor-bearing system. Among such factors one can enumerate external damping, rotor rigidity anisotropic factor, support rigidity anisotropic factor and the relative flexibility factor of the support. As a result of the analysis and numerical simulations it has been found that the rotor rigidity anisotropy and the system damping are the major factors contributing to the loss of stability of the system. To solve the issue of instability of the asymmetrical rotor-bearing system in engineering practice the authors have proposed a method aimed at enhancing the support rigidity symmetry of a rotor-bearing system, which has been proved effective in practice.

Key words: asymmetrical rotor-bearing system, stability analysis, rigidity, anisotropy

湍流焓传递方程及其应用 = Exergy Transfer Equation for Turbulent Flows and Its Applications [刊, 汉] / Wang Song-ping (Qingdao University, Qingdao, China, Post Code: 266071), Chen Qing-lin, Hua Ben (South China University of Science and Technology, Guangzhou, China, Post Code: 510641) // Journal of Engineering for Thermal Energy & Power. — 2001, 16(1). — 73 ~ 76

The authors have derived an exergy transfer equation for turbulent flows. On this basis a study was conducted of the exergy transfer for a convection heat exchange tube with a wall surface constant heat flux. The distribution of exergy loss rate caused by viscosity dissipation, radial and axial heat conduction was calculated. The calculation results of the total exergy loss rate for a unit volume indicate that the total exergy loss per unit volume is a multi-value function of heat exchange tube geometric parameters and boundary conditions. For a given geometric parameter there exists a boundary condition, which gives a minimum value of the total exergy loss rate for a unit volume, and vice versa. The above conclusion can to a certain extent serve as a guide for the optimized design of heat exchangers and the optimal selection of heat exchangers under given boundary conditions. **Key words:** turbulent flow, exergy transfer equation, distribution of exergy loss rate

某舰用锅炉过热器胀接头弹塑性有限元分析 = Finite Element Analysis of the Elastic Plasticity of a Naval Boiler Superheater Expanded-joint [刊, 汉] / Zhou Chuan-yue (Harbin Institute of Technology, Harbin, China, Post Code: 150001), Li Gui-ying, Ma Yun-xiang (Harbin No. 703 Research Institute, Harbin, China, Post Code: 150036) // Journal of Engineering for Thermal Energy & Power. — 2001, 16(1). — 77 ~ 79

Through the use of a large-sized finite element general program ANSYS the contact analysis model of an expanded joint has been set up for the expanded joint structure of a naval boiler superheater and a finite element analysis of three-dimensional plasticity conducted. A study was performed of the effect of material properties and operating temperatures, etc on the residual contact pressure of the expanded joint. Also given in this paper are some proposals, which can serve as a guide for engineering design as well as for the prevention of failures and malfunctions. **Key words:** expanded joint, finite element method (FEM), analysis of elastic plasticity, residual stress, program ANSYS

三维紊流燃烧室流场的数值计算 = Numerical Calculation of the Three-dimensional Turbulent Flow Field of a Gas Turbine Combustor [刊, 汉] / Xun Bai-qiu, Qu Zhe, Zhang Yanqiu, et al (Harbin No. 703 Research Institute, Harbin, China, Post Code: 150036) // Journal of Engineering for Thermal Energy & Power. — 2001, 16(1). — 80 ~ 82

By the use of a cylindrical coordinate system a numerical simulation was conducted of a single-tube return-flow combustor flow-field. A turbulent flow viscosity model was employed to evaluate the turbulent flow viscosity with the help of a $k-\epsilon$ dual equation turbulent flow model. A combustion model was utilized to assess chemical reaction speed with the help of a EBU (eddy-break-up) vortex breakage combustion model. Thermal radiation magnitude was calculated by using a thermal radiation model with the help of a relatively simple DTR (discrete transfer radiation) model. The results of the calculation have been found to reflect quite accurately the flow condition of the combustor flow field. Moreover, these results have al-